Smart Materials and Structures

PURPOSE-LED PUBLISHING™

PAPER • **OPEN ACCESS**

Antimicrobial thiol–acrylate vitrimers synthesized from glycerol and vanillin derivatives

To cite this article: Brigita Kazlauskaite *et al* 2025 *Smart Mater. Struct.* **34** 035044

View the article online for updates and enhancements.

You may also like

- Experimental study on the high-velocity impact resistance of Vitrimer-based carbon fiber composites
Ziyue Lin and Peng Chen
- Synthesis and Characterization of Vitrimer-like Self-Healing Polymer Electrolytes for Lithium Metal Batteries
Carla Barakat, He Jia and Jean-François Gohy
- Shape reconfiguration and functional self-healing of thermadapt shape memory epoxy vitrimers by exchange reaction of disulfide bonds
Ben Li, Guangming Zhu, Yujia Hao et al.

This content was downloaded from IP address 88.222.25.29 on 19/03/2025 at 13:47

OPEN ACCESS
IOP Publishing
Smart Materials and Structures
Smart Mater. Struct. **34** (2025) 035044 (11pp)
https://doi.org/10.1088/1361-665X/adbb98

Antimicrobial thiol–acrylate vitrimers synthesized from glycerol and vanillin derivatives

Brigita Kazlauskaite[1], Sigita Grauzeliene[1], Danguole Bridziuviene[2], Vita Raudoniene[2], Egidija Rainosalo[3] and Jolita Ostrauskaite[1,*]

[1] Department of Polymer Chemistry and Technology, Kaunas University of Technology, Kaunas 50254, Lithuania
[2] Biodeterioration Research Laboratory, Nature Research Center, Vilnius 08412, Lithuania
[3] Centria University of Applied Sciences, Kokkola 67100, Finland

E-mail: jolita.ostrauskaite@ktu.lt

Received 22 July 2024, revised 20 January 2025
Accepted for publication 28 February 2025
Published 11 March 2025

Abstract

This work presents innovations in polymer science through the development of antimicrobial and reprocessable shape-memory vitrimers from biobased vanillin and glycerol acrylates, incorporating pentaerythritol tetrakis(3-mercaptopropionate). The addition of this thiol increased the viscosity of the resin and reduced shrinkage and rigidity, without significantly affecting the polymerization rate. Samples containing 20 wt.% of thiol exhibited self-welding and 40% self-healing efficiency after just 10 min of heating at 180 °C and without additional pressure, significantly improving mechanical properties. The ability of vitrimers to maintain a temporary shape and return to a permanent shape under temperature changes showed shape-memory behavior, making them suitable for medicine, electronics, and robotics. The mechanical properties remained consistent after three reprocessing cycles, highlighting the sustainability of the vitrimers. The antimicrobial activity of these vitrimers showed efficacy up to 100%, suitable for antimicrobial films, coatings, and 3D printed parts. Microimprint lithography enabled micrometer-scale patterns, highlighting broad practical applications of the vitrimers.

Supplementary material for this article is available online

Keywords: vitrimer, vanillin, glycerol, biobased, shape-memory, reprocessing, antimicrobial

1. Introduction

The development of advanced functional polymers is of great interest due to the growing global concern about microbial contamination and the demand for sustainable materials [1, 2]. Vitrimers represent an innovative type of material distinguished by their remarkable capacity to undergo dynamic covalent exchange reactions while retaining a stable network structure [3–5]. These dynamic covalent bonds endow vitrimers with remarkable properties, including shape-memory, self-repair, and recyclability, making them highly attractive for a wide range of applications in various fields, including materials science [6–8]. The concept of vitrimers arises from the desire to combine the attributes of thermosetting polymers, such as high mechanical strength and chemical resistance, with the dynamic behavior of thermoplastics, which can

* Author to whom any correspondence should be addressed.

Original content from this work may be used under the terms of the Creative Commons Attribution 4.0 licence. Any further distribution of this work must maintain attribution to the author(s) and the title of the work, journal citation and DOI.

© 2025 The Author(s). Published by IOP Publishing Ltd

be reshaped and recycled [9, 10]. Traditional thermosetting polymers undergo irreversible curing reactions upon cross-linking, resulting in a fixed network structure that limits their processability and recyclability [11, 12]. In contrast, vitrimers are characterized by reversible exchange reactions between covalent bonds, allowing them to flow and rearrange under specific conditions while maintaining their structural integrity. The dynamic nature of vitrimers stems from the presence of dynamic covalent bonds, such as disulfide, imine, boronic ester bonds, and transesterification reactions [13–15]. These bonds allow vitrimers to undergo structural reconfiguration in response to external stimuli, such as heat, light, or pH [16]. As a result, vitrimers exhibit shape-memory behavior, self-repairing capabilities, and the ability to be reshaped, reprocessed, and recycled multiple times without significant degradation [17]. In particular, it is possible to program vitrimers to 'remember' a specific shape. They can change shape predeterminedly or return to their original shape when exposed to a triggering stimulus, e.g. heating. This ability to change shape on demand provides versatility since vitrimers can be molded into specific shapes during fabrication and then set to remember them. This enables the design of complex geometries tailored to specific applications. In addition, the responsiveness to external stimuli allows it to adjust to changing environmental conditions or mechanical loads [18–20]. Lastly, vitrimers can be reconfigured and reused in a variety of applications because of their ability to change shape without significant rupture. The adaptability provided by shape-memory properties allows vitrimers to be used in the development of smart materials and devices, such as self-actuating structures, shape-changing components, and adaptive surfaces [21, 22]. In general, vitrimers are adjusting materials, because their properties can be tailored and optimized for specific applications through adjustments in their chemical composition and processing techniques.

In this work, the synthesis and investigation of properties of new biobased and antimicrobial vitrimers were performed. Vanillin and glycerol acrylates were selected as raw materials in this study because of their significant advantages over traditional petrochemical-based monomers. Vanillin, derived from lignin, is not only a biobased material but also imparts inherent antimicrobial properties, making it a compelling choice for applications in environments where microbial resistance is essential, such as medical and food packaging materials. Additionally, glycerol acrylates, which can be synthesized from glycerol, a by-product of biodiesel production, offer a renewable alternative that improves polymer flexibility and reduces brittleness, addressing a common limitation in traditional vitrimer materials. Both vanillin and glycerol derivatives are safer than conventional alternatives such as bisphenol A, which poses health risks and contributes to environmental pollution. By incorporating these biobased acrylates, this study aims to develop vitrimers that combine antimicrobial activity, reprocessability, and structural flexibility with significant application potential in fields requiring recyclable and shape-memory polymers.

The purpose of this study was to develop vitrimers with antimicrobial properties using vanillin and glycerol acrylate fragments, to reduce the brittleness of the polymer and to increase the flexibility of the polymer as well as the number of ester functional groups in the vitrimer structure for reprocessability by using pentaerythritol tetrakis(3-mercaptopropionate) (PETMP). In addition, thiol–ene photopolymerization is attractive due to advantages such as rapid curing and low shrinkage [23]. For the first time, the photocuring kinetics and rheological properties of formulations containing acrylates based on glycerol and vanillin and PETMP were studied. The desired shape-memory, self-welding, self-healing, reprocessability, and antimicrobial properties were developed and compared to those of vitrimers based on bisphenol A glycerolate dimethacrylate (BisGMA). Sensors, robots, and computers have been reduced to millimeter or sub-millimeter sizes over the last decade. Such little machines are intelligent for numerous purposes, such as microsurgery or cargo transport [24]. Additionally, micrometer-scale patterns were successfully fabricated by microimprint lithography, filling the gap between high-resolution patterning and cost-effective manufacturing [25]. The great potential of the developed resins for this accurate, fast, easy, and inexpensive fabrication method was shown.

2. Experimental

2.1. Materials

Bisphenol A glycerolate dimethacrylate (BisGMA), 2-hydroxy-3-phenoxypropyl acrylate (HPPA), pentaerythritol tetrakis(3-mercaptopropionate) (PETMP), and 2,5-bis(5-tert-butylbenzoxazol-2-yl) thiophene (BBOT) were purchased from Merck, Darmstadt, Germany.2-Hydroxy-3-[[4-[2-hydroxy-3-[(2-methyl-1-oxo-2-propen-1-yl)oxy]propoxy]-3-methoxyphenyl]methoxy]propyl 2-methyl-2-propenoate (DGEVA dimethacrylate, DGEVADMA) was purchased from Specific Polymers, Castries, France. Ethyl(2,4,6-trimethylbenzoyl) phenylphosphinate (TPOL) was purchased from Fluorochem, Hadfield, UK. Miramer A99 was received from Miwon Europe GmbH, Mainz, Germany. All chemicals were used as received.

The vanillin-based monomer 2-hydroxy-3-[[4-[2-hydroxy-3-[(2-methyl-1-oxo-2-propen-1-yl)oxy]propoxy]-3-methoxyphenyl]methoxy]propyl 2-methyl-2-propenoate (DGEVA dimethacrylate, DGEVADMA) (figure 1) was chosen as a cross-linker for vitrimer synthesis due to the functional groups of hydroxyl and ester that are essential for transesterification reactions. DGEVA dimethacrylate can be produced from the second most abundant natural phenolic polymer lignin [26] and has a benzene ring in structure that provides high rigidity and thermal stability. As a result, it could be an alternative to bisphenol A-based monomers in vitrimeric synthesis, because bisphenol A is thought to contribute to metabolic and endocrine disorders, as well as to water pollution [27, 28]. Furthermore, vanillin-based polymers show antimicrobial properties [29, 30]. The monofunctional monomer 2-hydroxy-3-phenoxypropyl acrylate (HPPA) was selected as the most widely used monomer for vitrimer synthesis through transesterification reactions [31].

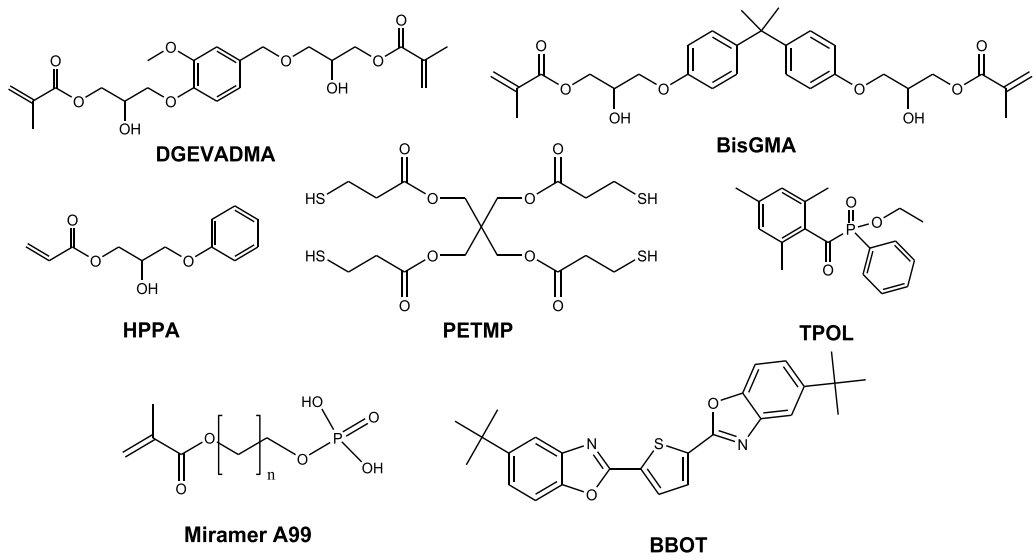

Figure 1. Chemical structures of 2-hydroxy-3-[[4-[2-hydroxy-3-[(2-methyl-1-oxo-2-propen-1-yl)oxy]propoxy]-3 -methoxyphenyl]methoxy]propyl 2-methyl-2-propenoate (DGEVADMA), bisphenol A glycerolate dimethacrylate (BisGMA), 2-hydroxy-3-phenoxypropyl acrylate (HPPA), pentaerythritol tetrakis(3-mercaptopropionate) (PETMP), ethyl(2,4,6-trimethylbenzoyl) phenylphosphinate (TPOL), Miramer A99, and 2,5-bis(5-tert-butyl-benzoxazol-2-yl)thiophene (BBOT).

Moreover, HPPA contains a fragment of glycerol, the primary building block of triglycerides, which can be obtained as a by-product of biodiesel production from vegetable and animal fats [32, 33]. Only partial recyclability has been obtained by using DGEVADMA [34]. The photoinitiator ethyl(2,4,6-trimethylbenzoyl)phenylphosphinate (TPOL) was used because of the photobleaching effect, which allows to obtain transparent product [35]. Miramer A99 was chosen as the transesterification catalyst due to its inertness in thiol-click formulations [31]. 2,5-Bis(5-tert-butyl-benzoxazol-2-yl)thiophene (BBOT) was used as a UV blocker to inhibit the premature photopolymerization of the formulations.

2.2. Preparation of UV/VIS-curable resins

The formulations were prepared by mixing 20 wt.% DGEVADMA or BisGMA with different amounts of HPPA and PETMP (table 1), and 0.08 wt.% of BBOT at 70 °C. PETMP was used up to 20% because increasing its concentration beyond this level resulted in poorer rheological and mechanical properties of the polymer samples. A higher thiol content made the samples brittle, making it difficult to remove them from the mold. When the formulations were cooled to room temperature, 3 mol.% of TPOL as a photoinitiator and 5 wt.% of Miramer A99 as the transesterification catalyst were added and stirred at room temperature.

Resin codes were denoted by a first letter of either DGEVADMA or BisGMA, a number that indicated the amount of PETMP, and the first letter of PETMP, e.g. D-20P denotes a resin with 20 wt.% of DGEVADMA, 60 wt.% of HPPA, and 20 wt.% PETMP.

Viscosity of the resins was measured using an Anton Paar MCR302 rheometer (Graz, Austria) equipped with a plate/-plate accessory (15 mm diameter of the upper plate), employing shear rates ranging from 0.001 to 50 s^{-1} at a temperature of 25 °C.

The resins were then subjected to UV/VIS curing in a Teflon mold ($70 \times 10 \times 1$) $\pm$ 0.01 mm under a 100 W Helios Italquartz GR.E UV lamp emitting light at a wavelength of 250–450 nm and an intensity of 310 mW cm^{-2} for 2 min until a solid polymer was formed.

2.3. Self-welding experiment

The UV/VIS-cured samples, measuring ($10 \times 10 \times 1$) $\pm$ 0.01 mm, were halved, then aligned and joined together before being subjected to heating at 180 °C for 10 min. Elevated temperatures facilitate the dynamic covalent exchanges critical to self-healing. Subsequently, the rejoined samples were mechanically tested using a Testometric M500-50CT machine (Testometric Co, Ltd, Rochdale, UK).

2.4. Self-healing experiment

The scratch repair test was carried out by scratching the UV/VIS-cured vitrimer sample with a razor blade, curing at 180 °C for 1 h and then analyzing with a Hitachi SEM TM4000 II (Hitachi High-Tech Corporation, Hitachi Europe Ltd). The self-healing efficiency was calculated as the ratio between the width of scratch before and after repair.

Table 1. Composition and viscosity of resins.

Resin	Amount of DGEVADMA or BisGMA (wt.%)	Amount of HPPA (wt.%)	Amount of PETMP (wt.%)	Viscosity (mPa·s)
D-0P		80	0	511 ± 1
D-5P		75	5	537 ± 3
D-10P	20	70	10	604 ± 8
D-15P		65	15	621 ± 9
D-20P		60	20	705 ± 5
B-0P		80	0	513 ± 4
B-5P		75	5	585 ± 3
B-10P	20	70	10	607 ± 3
B-15P		65	15	629 ± 3
B-20P		60	20	708 ± 2

2.5. Shape-memory experiments

Samples with dimensions of (70 × 10 × 1) ± 0.01 mm were welded into a gripper and used for shape-memory experiments. The sample was mechanically deformed at room temperature from its permanent form to the desired shape to take the plug and cooled below T_g as shown in figure 7.

The shape recovery ratio (RR) was determined by comparing the polymer's lengths at various stages of the shape memory process. Initially, the sample was heated to 90 °C (above the T_v) and stretched by applying a force. During the fixing stage, the sample was cooled to room temperature while maintaining the applied load, and then the tensile load was released. Finally, the deformed sample was reheated to 90 °C, allowing it to recover its original length. RR was calculated according to the equation:

$$\mathrm{RR} = \frac{L_f - L}{L_f - L_0} \quad (1)$$

where RR is the shape recovery ratio (%), L_0 is the original length of the sample (cm), L_f is the length of the sample in the fixing stage after releasing the tensile load (cm), and L is the length of the sample in the recovery stage when heated to 90 °C (cm).

2.6. Reprocessability experiments

The photocured samples were purged with liquid nitrogen, grinded and compressed in a mould (50 × 70 × 1) mm at 210 °C for 25 min under a pressure of 4 metric tons on a Carver hot press (Carver Inc., Wabash, IN, USA). After being cooled to room temperature, the mechanical properties of the reprocessed samples were tested using a TIRA test 2705 machine (TIRA GmbH, Schalkau, Germany). The average of 3 parallel measurements was calculated and the variation of the experimental results did not exceed 5% within the group.

2.7. Antimicrobial experiments

The study of the antimicrobial activity of polymers was carried out using the methodology described in a previous publication [29]. The concentrations of the microbial inoculum were 1.9×10^6, 2.3×10^7, and 1.0×10^8 colony forming units ml^{-1} (CFU ml^{-1}) for *Escherichia coli (E. coli)*, 2.35×10^7 for *Staphylococcus aureus* (*S. aureus*), 8.50×10^6 for *Aspergillus flavus* (*A. flavus*), and 3.95×10^6 for *Aspergillus niger* (*A. niger*). Ten microliter of the bacterial or fungal suspension was applied to the surface of the test films (10 × 10 mm) and incubated in a humid chamber (90% relative humidity) at 37 °C in the case of infection with bacteria and at 26 °C in the case of infection with fungi for 1, 2 and 4 h. The percentage reduction of viable microbial spores was calculated according to the formula: $(a - b)/a \cdot 100\%$, where a is the concentration of the colony forming units (CFU ml^{-1}) in inoculum suspension; b is a mean of viable spores (CFU ml^{-1}) on samples from triplicate experiments after incubation.

2.8. Microimprint lithography

An Asiga Pico2 39 UV table-top 3D printer (Asiga) was used to produce a 1951 USAF resolution test target structure out of PlasGray material. Polydimethylsiloxane (PDMS) was then poured over the target structure and thermally cured at 100 °C for 1 h, resulting in a soft mold that was used to make replicas. The resins were cured under a 100 W Helios

Italquartz GR.E UV lamp that emits light at a wavelength of 250–450 nm and an intensity of 310 mW cm^{-2} for 2 min.

2.9. Characterization techniques

Characterization methods are described in the Supplementary Information.

3. Results and discussions

3.1. Kinetics of photocuring

Real-time photorheometry was used to monitor the viscoelastic behavior and rheological characteristics including viscosity, shrinkage, and rigidity of the resins after applying UV/Vis light irradiation. When PETMP was added, the viscosity increased in the resins containing DGEVADMA and

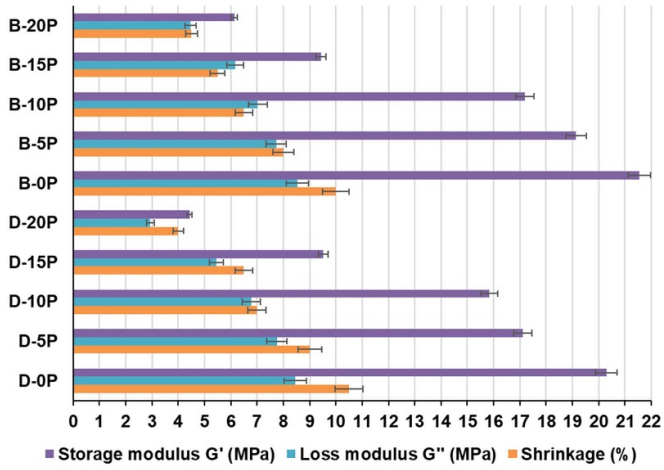

Figure 2. Photorheometric characteristics.

BisGMA due to the higher viscosity of PETMP compared to the monomer HPPA, and ranged from 511 to 708 mPa·s (table 1). The viscosity of the bisphenol A diacrylate-containing resins was slightly higher compared to that of the vanillin diacrylate-containing resins as a result of the higher viscosity of BisGMA.

The addition of the UV blocker BBOT did not significantly change the viscosity and prevented prepolymerization of the resins; after a month in the dark, the change was less than 5%. After exposure to UV/Vis for 1 s, all resins reached the gel point, which means that the addition of PETMP did not affect the rate of polymerization and the reaching of the plateau of G' and G'' modules. For example, the resin D-0P had G' and G'' modules of 20.29 MPa and 8.45 MPa, respectively, after 120 s of irradiation (figure 2). The values reached for the G' and G'' modules were slightly higher compared to those of the resin composed of DGEVADMA and HPPA (13.55 MPa and 6.16 MPa, respectively) [34] and using different transesterification catalyst, since Miramer A99 was covalently incorporated into the network through its methacrylate group. All rheological parameters, such as G' and G'' modules (figure S1(a) and (b), and shrinkage were reduced by increasing the amount of PETMP to 20% by weight. At higher PETMP concentrations, the thiol–ene step growth process is dominated rather than the chain-growth mechanism of acrylate monomers, resulting in lower resin shrinkage and rigidity of the polymer. The reduction in the G' and G'' modules curves of some resins was observed because of softening of the polymers regarding the plasticization of the polymer matrix when exposed to UV/Vis light.

Thiol PETMP acted as a chain transfer agent by reducing shrinkage, resulting in a uniform polymer structure that is a function of the photopolymerization step-growth process [36]. However, the values of the rheological parameters of DGEVADMA were slightly lower than those of BisGMA resins, but of the same magnitude due to the lower viscosity and one aromatic ring compared to two rings of BisGMA.

3.2. Mechanical properties

The mechanical characteristics of the photo-cured resins were examined by tensile testing of the polymer samples (figure S2). The incorporation of PETMP resulted in a decrease in Young's modulus and the tensile strength values which correlated with the storage modulus G' values from photorheometric studies and may be due to the lower yield of the insoluble fraction. The polymer without PETMP had Young's modulus of 8.99 MPa, which was similar to that of the DGEVADMA and HPPA polymer synthesized using another catalyst (5.69 MPa) [34]. The elongation at break was the highest when 5 wt.% of PETMP was used and decreased with increasing amounts of it. The B-5P polymer exhibited more than twice as much elongation at break than its analogue with the vanillin diacrylate fragments D-5P. The values of Young's modulus and tensile strength of samples with bisphenol A diacrylate fragments were slightly higher but in the same magnitude as those of polymers with vanillin diacrylate fragments, may be due to the two aromatic rings in the structure.

3.3. Self-welding properties

Unlike traditional thermosets, vitrimers having dynamic covalent bonds enable welding through thermally activated bond exchange reactions, providing ecological and economic benefits. Self-welding can extend the lifespan of materials and reduce energy consumption for the production of new materials. Above the topology freezing temperature, dynamic transesterification reactions are activated, and the results of self-welding are noticeable. Only samples D-20P and B-20P with the highest concentration of PETMP showed self-welding properties. In these samples, not only the covalent bonds formed, but also the greater amount of –SH and C=O groups present in the PETMP fragment could impart the hydrogen bonding between the polymer chains [36, 37]. Therefore, the determination of the T_v of the vitrimers D-20P and B-20P is shown in figures 3(a) and (b). Vitrimers can relieve stress at high temperatures ranging from 160 °C to 220 °C through dynamic cross-link exchange reactions. Relaxation time (τ) was determined as the time needed to relax to $1/e$ (36.8%) of the initial stress [38]. The relaxation time increased as the temperature decreased for both vitrimers. In the case of vitrimer D-20P with vanillin diacrylate fragments, τ ranged from 17 min to 3 min, while in the case of vitrimer B-20P with bisphenol A diacrylate fragments, τ ranged from 132 min to 8 min, demonstrating fast stress relaxation. The τ values were plotted as a function of temperature and T_v was determined by extrapolating the fitted line. The T_v of the vitrimers was determined to be 9 °C and 84 °C (figure 3(b)). Such a low T_v value of D-20P shows the extremely fast stress relaxation. This shows that vitrimer D-20P with vanillin diacrylate fragments had a more efficient rearrangement of polymer chains compared to vitrimer B-20P due to one aromatic ring that could impart a fast exchange reaction of dynamic cross-links [39].

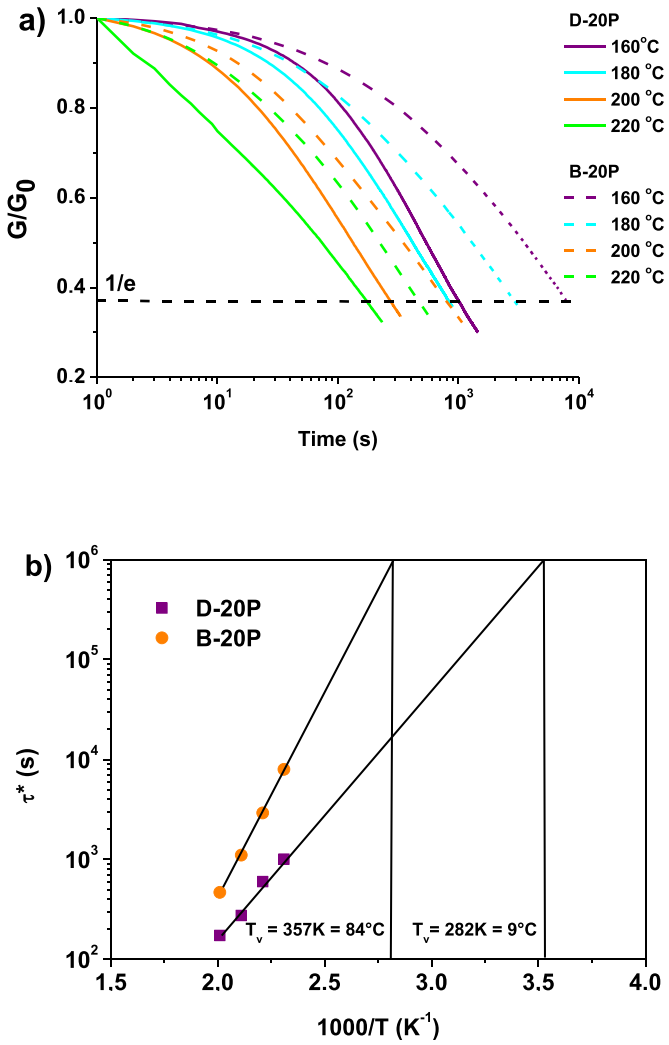

Figure 3. Stress relaxation curves versus time (a) and the Arrhenius plot of relaxation times (b).

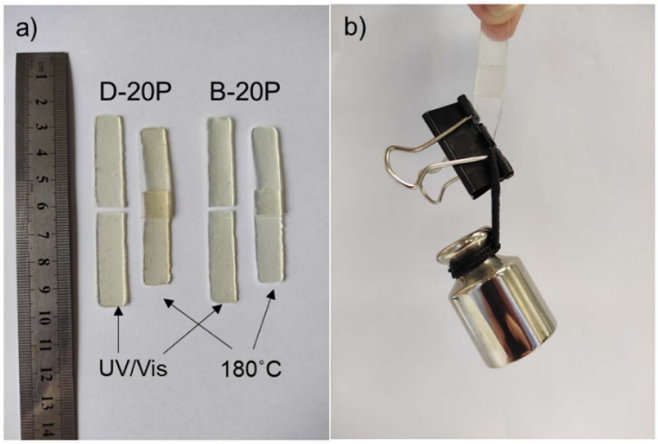

Figure 4. A photograph of vitrimers obtained by UV/VIS-curing and after self-welding at 180 °C (a), and a photograph of self-welded D-20P that holds a weight of 500 g (b).

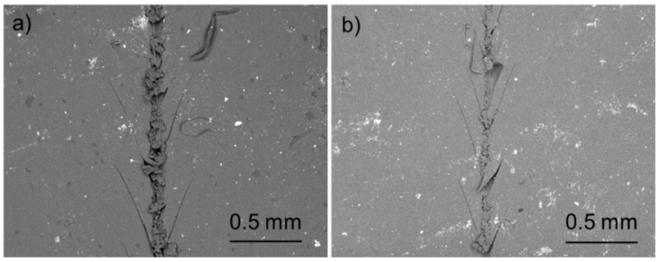

Figure 5. SEM images of the scratch sample D-20P (a) and the same sample cured at 180 °C for 1 h (b).

To show self-welding properties, the rectangular sample obtained after photopolymerization was cut in half, adhered together placing 1 × 1 cm pieces on top of each other, and heated to 180 °C only for 10 min (figure 4(a)). The optimal thiol content to ensure the self-welding properties of the polymers is 20 wt.% in both polymer series containing

Vanillin diacrylate and bisphenol A diacrylate fragments. After welding, the vitrimer samples were able to hold a weight of 500 g (figure 4(b)). The mechanical parameters of the original and welded samples were compared.

After heating at a temperature of 180 °C, the polymer sample with the vanillin diacrylate fragments showed about 4.5 times higher tensile strength and approximately 1.6 times higher Young's modulus values. Tensile strength and Young's modulus values of the heated polymer sample containing bisphenol A diacrylate fragments increased approximately 2.5 times. The reason for the increased mechanical characteristics could be the additional formation of hydrogen bonds during curing at 180 °C. The lifespan and sustainability of the vitrimer could be enhanced by weldability using 20 wt.% of thiol in the resin only after 10 min of heating at 180 °C. Vitrimers with 20 wt.% of PETMP were selected to test their shape-memory, reprocessability, and antimicrobial properties.

3.4. Self-healing properties

The repair of thermosets is impossible, which leads to a lot of waste and costs. Potential replacement of thermosets is vitrimers with self-healing properties. To confirm the repairability of the UV/VIS-cured sample D-20P, a scratch-repair test was performed. Figure 5 shows SEM images of a UV/VIS-cured sample that was scratched with a razor blade and repaired at 180 °C for 1 h. Side scratches and folds were formed in addition to the main scratch due to the usage of a razor blade. When the vitrimer is damaged, reversible exchange reactions of covalent bonds occur under heating conditions, allowing the sample to rearrange its molecular structure and repair damage. The scratch became less obvious in the D-20P sample, indicating good self-healing properties. The self-healing efficiency of 40% was obtained as the ratio between the width before and after the repair. The ability of the vitrimer to undergo reversible bond exchange enabled it to exhibit self-healing properties, making it a promising candidate for applications where durability and longevity are crucial.

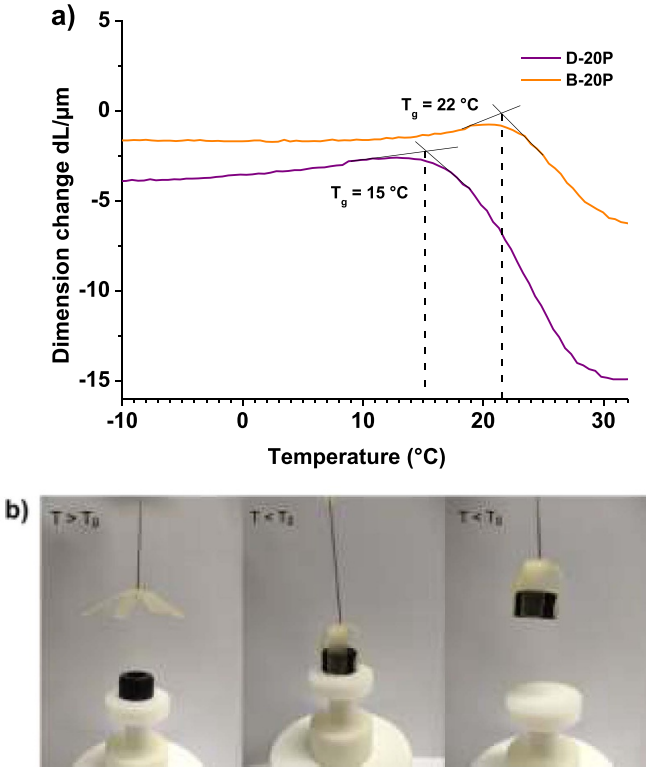

Figure 6. Dimensional change curves of the vitrimers D-20P and B-20P (a) and photographs expressing the monitoring of the shape-memory behavior of the D-20P 'gripper' sample (b).

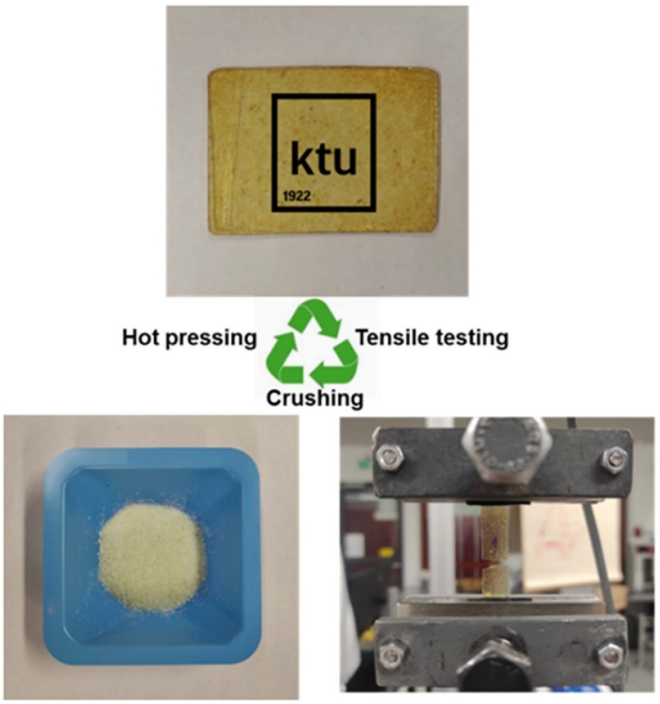

Figure 7. Scheme expressing the reprocessability experiment.

3.5. Shape-memory properties

One of the advantages of vitrimers is that they can change their shape permanently as a result of their ability to maintain a temporary shape and return to a permanent shape under temperature changes. Shape change and memory were tested with a self-welded 'gripper' sample below its T_g. The T_g of the D-20P and B-20P vitrimers, defined from the dimensional change curve (figure 6(a)), was 15 °C and 22 °C, respectively. Two aromatic rings of bisphenol A diacrylate slightly increased the glass transition of the polymer compared to that of the polymer containing vanillin diacrylate fragments with only one aromatic ring. As shown in figure 6(b), the sample D-20P, which was in its permanent form at room temperature, was mechanically deformed to the desired shape to take the plug shown in the photo and cooled below T_g. The sample was able to change its permanent shape to the desired shape and retain the plug shown in the photo because of the plasticity of the free hydroxyl groups and branched macromolecules with aromatic ring and aliphatic chains. When the sample was heated to room temperature, it quickly recovered after 3 s to a permanent shape. Both the D-20P and B-20P samples showed a shape RR of 100%, indicating that the samples are able to recover their original length. The shape-memory behavior of D-20P vitrimer makes it a good candidate for medicine, electronics, and multifunctional robotic systems.

3.6. Reprocessability of polymers

Following confirmation of the stress relaxation behavior of the vitrimers, the reprocessability provided by the dynamic covalent network was examined. D-20P and B-20P should be easily reprocessed at high temperatures due to their low relaxation time. Figure 7 illustrates how crushed vitrimer samples can be molded into rectangles using a hot press machine at 210 °C for 25 min at 4 metric tons. More notably, even after three hot-press reprocessing cycles, both reprocessed vitrimers maintained the same level of mechanical properties (figure S3) or showed even higher values, which are crucial for the practical application of vitrimers.

Furthermore, the intensities of the OH and C=O group signals at 3490 cm^{-1} and 1740 cm^{-1}, respectively, in the FT-IR spectra after reprocessing were identical to those of the original samples (figure S4). This was due to the dynamic transesterification reaction that occurred during reprocessing. Exchangeable hydroxyl groups and ester groups can be released at high temperatures when nucleophilic hydroxyl groups react with the ester group to generate an associate intermediate [40]. Additionally, thermogravimetric analysis showed that these vitrimers were thermally stable at 210 °C under the conditions tested (figure S5). Synthesized vitrimers D-20P and B-20P can be recycled from their waste materials, according to the reprocessability experiment, thus highlighting their sustainability and potential for circular economy practices in material science.

Table 2. Antimicrobial characteristics of vitrimers.

Vitrimer	Time (h)	Reduction in microbial spores (CFU ml^{-1}) (%)			
		E. coli	*S. aureus*	*A. flavus*	*A. niger*
D-20P	1	99.97 ± 0.01	99.6 ± 0.12	86.2 ± 0.05	72.1 ± 0.06
	2	100 ± 0.00	100 ± 0.00	93.0 ± 0.06	65.5 ± 0.09
	4	100 ± 0.00	100 ± 0.00	93.2 ± 0.01	68.7 ± 0.02
B-20P	1	96.16 ± 0.59	61.8 ± 0.02	92.2 ± 0.12	78.8 ± 0.01
	2	99.99 ± 0.01	100 ± 0.00	92.2 ± 0.04	68.0 ± 0.01
	4	100 ± 0.00	100 ± 0.00	88.0 ± 0.01	77.0 ± 0.01

3.7. Antimicrobial properties

The antibacterial and antifungal properties of the D-20P and B-20P vitrimer films were tested in direct contact of the bacterial or fungal suspensions with specimens and by calculating the percentage reduction of viable microbial spores. The results are shown in table 2 and figure 8. Both vitrimers showed antimicrobial activity against all tested microorganisms, with *A. niger* generally being the most viable and *E. coli* the most susceptible, as *E. coli* has a simple cell structure without membrane-bound organelles, while *A. niger* has organelles such as nucleus, mitochondria, and endoplasmic reticulum [41]. In both vitrimer cases, the percentage reduction of viable microbial spores increased with time. However, D-20P exhibited a higher percentage of bacteria reduction after 1 h compared to B-20P, indicating that DGEVADMA had more effective antibacterial activity compared to BisGMA. After 2 h of exposure to D-20P, *E. coli* and *S. aureus* spores were reduced to 100%, while *A. flavus* spores were reduced to 93.0% and *A. niger* to 65.5%. Similarly, after 4 h of exposure, the reduction of bacteria spores remained 100% and the reduction of fungal spores increased to 93.2% and 68.7%, respectively. However, in the case of exposure to B-20P, the reduction of *A. flavus* spores was reduced after 4 h compared to the reduction after 2 h. This could be explained by the development of vegetative cells from spores under the appropriate conditions. Both vitrimers have hydroxyl, sulfur, and carbonyl groups that contribute to the antimicrobial effect [26, 42, 43]. Hydroxyl groups may enhance interactions with components of the microbial cell wall, resulting in membrane rupture. Components of the microbial cell wall can form hydrogen bonds with carbonyl groups, which can destabilize the membrane. Additionally, thiols have antimicrobial activities by creating disulfide bonds with cysteine residues in microbial proteins, altering their structure and function.

Bacterial *E. coli* infections are among the leading causes of death in hospitals worldwide, as bacteria can grow on a variety of surfaces, such as urine catheters and heart valves [44]. Bacteria also grow in materials used in wearable electronics, textile products, etc. One of the possible ways to deal with these problems is the use of antimicrobial film coatings on medical and electronic equipment, and the research and development of antibacterial polymer films is critical to prevent bacterial multiplication. Therefore, the antibacterial activity of the vitrimer films was investigated after 1 h using different concentrations of *E. coli* inoculum. The results are presented in figure 9. Vitrimer D-20P with vanillin diacrylate fragments reduced cell growth by 100% at concentrations of $1.9 \cdot 10^6$ and $2.3 \cdot 10^7$ CFU ml^{-1} and by 99% at a higher concentration of $1.0 \cdot 10^8$ CFU ml^{-1} even after 1 h of contact with bacteria. These values are similar to vitrimers with typical antimicrobial agents, such as alkyl-substituted quaternary ammonium groups (86%–99%) [45, 46]. However, cell reduction by vitrimer B-20P with the bisphenol A diacrylate fragments was 100% only at a lower concentration of $1.9 \cdot 10^6$ CFU ml^{-1} and continued to decrease to 48% at the highest concentration of $1.0 \cdot 10^8$ CFU ml^{-1}. The methoxy group is considered to have excellent antibacterial activity [47]. In this study, the methoxy group of the vanillin fragment was found to have the greatest impact on the reduction of *E. coli* cells compared to the aromatic structure of the bisphenol A fragment and the sulfur groups of PETMP fragments. It was previously found that vanillin treatment can damage the membrane structure of *E. coli*, resulting in leaks of nucleic acids and proteins within the cell. Furthermore, vanillin treatment reduces the concentration of adenosine triphosphate (ATP) in *E. coli* cells, causing cell death [48]. The results of antimicrobial activity highlight the potential of vitrimers containing vanillin diacrylate fragments as effective antimicrobial films or 3D printed objects against infections.

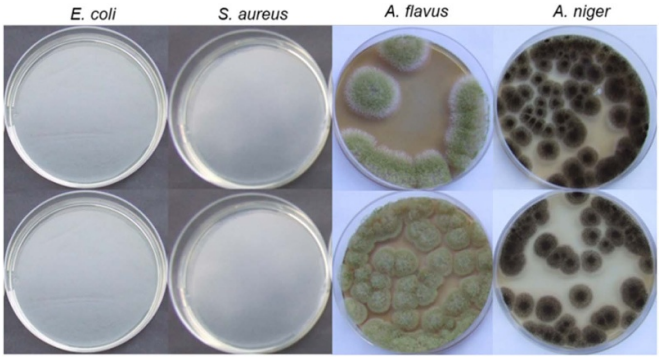

Figure 8. Photos of the resulting suspensions plated on nutrient media after 4 h: top Petri dishes—D-20P, bottom—B-20P.

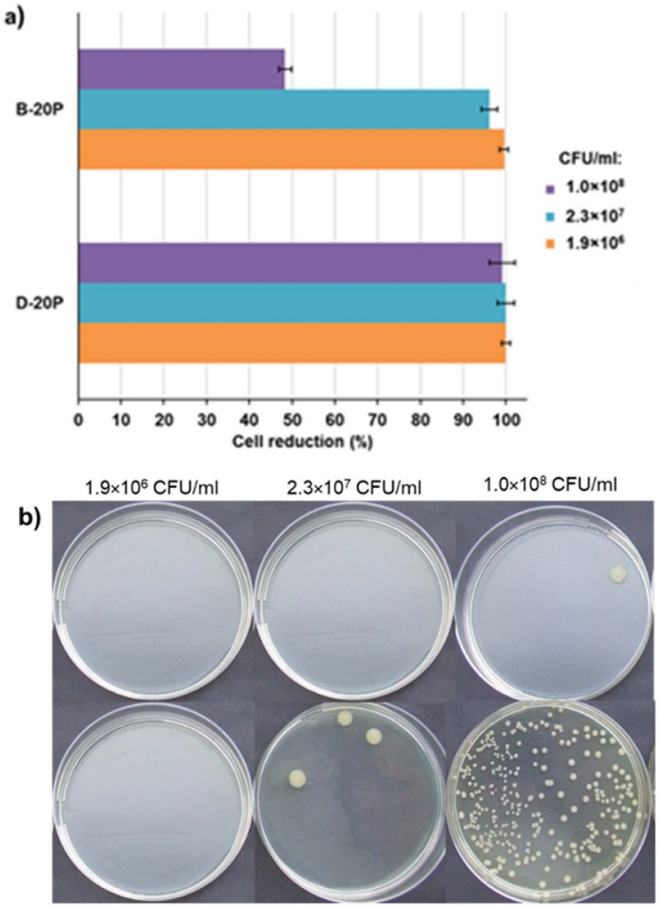

Figure 9. Reduction of *E. coli* cells during 1 h of contact time with the vitrimers containing fragments of vanillin diacrylate and bisphenol A diacrylate (a) and photos of the resulting suspensions plated on nutrient media (b): top Petri dishes—D-20P, bottom—B-20P.

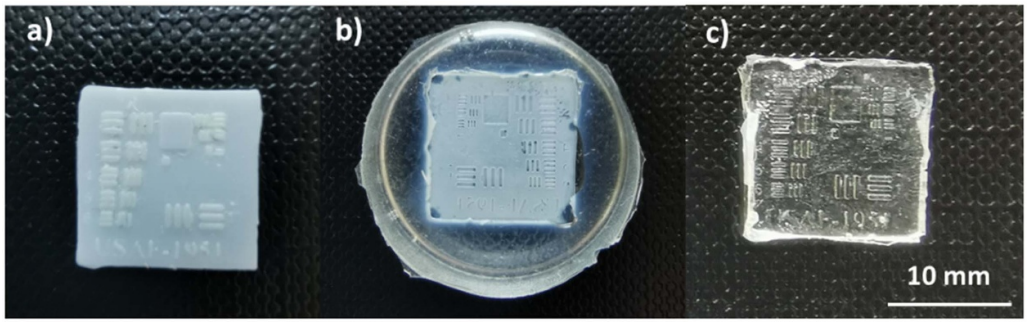

Figure 10. Photos taken during the microimprint lithography test include a 3D printed 1951 USAF target (a), a PDMS mold (b), and a replica made of resin D-20P (c).

3.8. Microimprint lithography testing

Resin D-20P was tested in microimprint lithography, which is used to produce patterns with high resolution and precision, and it is widely used in various applications, including electronics, optics, biotechnology, and surface engineering [23, 49]. Photos taken during the testing are presented in figure 10. The D-20P resin replica matched the PDMS mold in shape and details (letters and numbers): the thinnest line of 69 μm width and the thickest of about 220–230 μm width were obtained. The replica had only minor defects, such as the loss of sharp edges caused by the peeling of the stamp. The D-20P resin showed great potential to be used for microimprint lithography as thin features with high precision were produced.

4. Conclusions

UV/VIS-curable transesterification vitrimers containing fragments of vanillin-based diacrylate, glycerol-based acrylate, bisphenol A diacrylate, and pentaerythritol tetrakis(3-mercaptopropionate) were developed and mechanical,

thermal, self-welding, self-healing, shape-memory, reprocessability, and antimicrobial properties were investigated. The addition of pentaerythritol tetrakis(3-mercaptopropionate) did not affect the polymerization rate, but reduced the values of the rheological characteristics. Mechanical tests showed a decrease in Young's modulus and tensile strength values with the addition of pentaerythritol tetrakis(3-mercaptopropionate), while the elongation at break was the highest with 5 wt.% of pentaerythritol tetrakis(3-mercaptopropionate). Among the most important findings is that self-welding capability was observed with 20 wt.% of pentaerythritol tetrakis(3-mercaptopropionate) after just 10 min of heating at 180 °C and without additional pressure, resulting in significant improvement in mechanical properties after heating. The synthesized vitrimer showed self-healing with an efficiency of 40%. Shape-memory behavior enabled permanent shape change and recovery at temperatures above and below the glass transition temperature. Excellent reprocessability, with mechanical properties maintained over three reprocessing cycles, demonstrated the suitability of vitrimers for circular economy practices. Antimicrobial testing has revealed superior efficacy of the vitrimer with vanillin diacrylate fragments compared to an analogue containing bisphenol A diacrylate fragments. The resin with 20 wt.% of pentaerythritol tetrakis(3-mercaptopropionate) demonstrated high precision and potential for use in microimprint lithography, producing detailed replicas. These findings highlight the multidimensional applicability of innovative vitrimers with incorporated pentaerythritol tetrakis(3-mercaptopropionate) fragments, which provide variable material characteristics for a wide range of industrial and biomedical applications, including textile products, electronics, robotics, and antimicrobial films, coatings, or 3D printed objects.

Data availability statement

All data that support the findings of this study are included within the article (and any supplementary files).

Acknowledgment

This research was funded by the Research Council of Lithuania (project No. S-MIP-23-52).

The Chemistry and Bioeconomy team at the Centria University of Applied Sciences is gratefully acknowledged for their invaluable support, including guidance on materials testing and access to equipment.

Professor Dr M Malinauskas and Dr E Skliutas from the Laser Research Center, Faculty of Physics, Vilnius University, are gratefully acknowledged for the 3D printed target used in the microimprint lithography test.

Conflict of interest

The authors declare no conflict of interest.

Author contributions

B K contributed to formal analysis, investigation. S G—conceptualization, methodology, formal analysis, investigation, writing—original draft. D G—methodology, formal analysis, investigation. V R—methodology, formal analysis, investigation. E R—methodology, conceptualization, supervision. J O—methodology, conceptualization, supervision, writing—review & editing.

ORCID iDs

Sigita Grauzeliene https://orcid.org/0000-0003-1953-1074
Jolita Ostrauskaite https://orcid.org/0000-0001-8600-7040

References

[1] Li P, Zhang J, Ma J, Xu C A, Liang X, Yuan T, Hu Y and Yang Z 2023 Fully bio-based thermosetting polyimine vitrimers with excellent adhesion, rapid self-healing, multi-recyclability and antibacterial ability *Ind. Crops Prod.* **204** 117288
[2] Chen B, Lai G, Liu Z, Luo W, Lin S, Zhang H and Chen M 2023 Silicon-bridged epoxy vitrimers with antibacterial and UV-blocking properties *Appl. Polym. Mater.* **5** 6421–8
[3] Van Zee N J and Nicolaÿ R 2020 Vitrimers: permanently crosslinked polymers with dynamic network topology *Prog. Polym. Sci.* **104** 101233
[4] Zheng J, Png Z M, Ng S H, Tham G X, Ye E, Goh S S, Loh X J and Li Z 2021 Vitrimers: current research trends and their emerging applications *Mater. Today* **51** 586–625
[5] Guerre M, Taplan C, Winne J M and Du Prez F E 2020 Vitrimers: directing chemical reactivity to control material properties *Chem. Sci.* **11** 4855–70
[6] Hornat C C and Urban M W 2020 Shape memory effects in self-healing polymers *Prog. Polym. Sci.* **102** 101208
[7] Joe J *et al* 2021 A 4D printable shape memory vitrimer with repairability and recyclability through network architecture tailoring from commercial poly (ε-caprolactone) *Adv. Sci.* **8** 2103682
[8] Li Z, Yu R and Guo B 2021 Shape-memory and self-healing polymers based on dynamic covalent bonds and dynamic noncovalent interactions: synthesis, mechanism, and application *ACS Appl. Bio Mater.* **4** 5926–43
[9] Lucherelli M A, Duval A and Avérous L 2022 Biobased vitrimers: towards sustainable and adaptable performing polymer materials *Prog. Polym. Sci.* **127** 101515
[10] Alabiso W and Schlögl S 2020 The impact of vitrimers on the industry of the future: chemistry, properties and sustainable forward-looking applications *Polymers* **12** 1660
[11] Jia Y, Xie H, Qian J, Zhang Y, Zheng H, Wei F, Li Y and Zhao Z 2024 Recent progress on the 3D printing of dynamically cross-linked polymers *Adv. Funct. Mater.* **34** 2307279
[12] Jarach N, Dodiuk H, Kenig S and Magdassi S 2023 Fully recyclable cured polymers for sustainable 3D printing *Adv. Mater.* **36** 2307297
[13] Zhang Y, Ma F, Shi L, Lyu B and Ma J 2023 Recyclable, repairable and malleable bio-based epoxy vitrimers: overview and future prospects *Curr. Opin. Green Sustain. Chem.* **39** 100726
[14] Anagwu F I, Thakur V K and Skordos A A 2023 High-performance vitrimeric benzoxazines for sustainable

advanced materials: design, synthesis, and applications *Macromol. Mater. Eng.* **308** 2200534
[15] Stewart K A, Lessard J J, Cantor A J, Rynk J F, Bailey L S and Sumerlin B S 2023 High-performance polyimine vitrimers from an aromatic bio-based scaffold *RSC Appl. Polym.* **1** 10–18
[16] Kuang X, Mu Q, Roach D J and Qi H J 2020 Shape-programmable and healable materials and devices using thermo-and photo-responsive vitrimer *Multifunct. Mater.* **3** 045001
[17] Chen L, Li Z, Ma Y, Shang Q, Hu Y, Huang Q, Zhang M, Jia P and Zhou Y 2023 Tung oil-based degradable vitrimer for reprocessable and recyclable vitrimer–MWCNT composites with self-healing ability triggered by multiple stimuli *ACS Appl. Polym. Mater.* **5** 9203–12
[18] Hu L, Wan Y, Zhang Q and Serpe M J 2020 Harnessing the power of stimuli-responsive polymers for actuation *Adv. Funct. Mater.* **30** 1903471
[19] Zhang Q, Zhang Y, Wan Y, Carvalho W, Hu L and Serpe M J 2021 Stimuli-responsive polymers for sensing and reacting to environmental conditions *Prog. Polym. Sci.* **116** 101386
[20] Biswas M C, Chakraborty S, Bhattacharjee A and Mohammed Z 2021 4D printing of shape memory materials for textiles: mechanism, mathematical modeling, and challenges *Adv. Funct. Mater.* **31** 2100257
[21] Ryan K R, Down M P and Banks C E 2021 Future of additive manufacturing: overview of 4D and 3D printed smart and advanced materials and their applications *Chem. Eng. J.* **403** 126162
[22] Krishnakumar B, Sanka R P, Binder W H, Parthasarthy V, Rana S and Karak N 2020 Vitrimers: associative dynamic covalent adaptive networks in thermoset polymers *Chem. Eng. J.* **385** 123820
[23] Hoyle C E and Bowman C N 2010 Thiol–ene click chemistry *Angew Chem. Int. Ed.* **49** 1540–73
[24] Bandari V K and Schmidt O G 2021 System-engineered miniaturized robots: from structure to intelligence *Adv. Intell. Syst.* **3** 2000284
[25] Unno N and Mäkelä T 2023 Thermal nanoimprint lithography—a review of the process, mold fabrication, and material *Nanomaterials* **13** 2031
[26] Kumar B, Agumba D O, Pham D H, Latif M, Dinesh K, Kim H C, Alrobei H and Kim J 2021 Recent research progress on lignin-derived resins for natural fiber composite applications *Polymers* **13** 116
[27] Rochester J R, Bolden A L and Kwiatkowski C F 2018 Prenatal exposure to bisphenol A and hyperactivity in children: a systematic review and meta-analysis *Environ. Int.* **114** 343–56
[28] Onundi Y *et al* 2017 A multidisciplinary investigation of the technical and environmental performances of TAML/peroxide elimination of bisphenol A compounds from water *Green Chem.* **19** 4234–62
[29] Navaruckiene A, Bridziuviene D, Raudoniene V, Rainosalo E and Ostrauskaite J 2022 Vanillin acrylate-based thermo-responsive shape memory antimicrobial photopolymers *Express Polym. Lett.* **16** 279–95
[30] Motiekaityte G, Navaruckiene A, Raudoniene V, Bridziuviene D, Jaras J, Kantminiene K and Ostrauskaite J 2023 Antimicrobial dual-cured photopolymers of vanillin alcohol diglycidyl ether and glycerol dimethacrylate *J. Appl. Polym. Sci.* **140** e53289
[31] Rossegger E, Höller R, Reisinger D, Strasser J, Fleisch M, Griesser T and Schlögl S 2021 Digital light processing 3D printing with thiol–acrylate vitrimers *Polym. Chem.* **12** 639–44
[32] Quispe C A, Coronado C J and Carvalho J A Jr 2013 Glycerol: production, consumption, prices, characterization and new trends in combustion *Renew. Sustain. Energy Rev.* **27** 475–93
[33] Yang F, Hanna M A and Sun R 2012 Value-added uses for crude glycerol–a byproduct of biodiesel production *Biotechnol. Biofuels* **5** 13
[34] Grauzeliene S, Kastanauskas M, Talacka V and Ostrauskaite J 2022 Photocurable glycerol-and vanillin-based resins for the synthesis of vitrimers *ACS Appl. Polym. Mater.* **4** 6103–10
[35] Green W A 2010 *Industrial Photoinitiators: A Technical Guide* (CRC Press)
[36] Shi Q, Jin C, Chen Z, An L and Wang T 2023 On the welding of vitrimers: chemistry, mechanics and applications *Adv. Funct. Mater.* **33** 2300288
[37] Gong L, Wang S, Hu J, Feng H, Zhang L, Dai J and Liu X 2023 A novel bio-based degradable, reinforced vitrimer regulated by intramolecular hydrogen bonding *Prog. Org. Coat.* **175** 107384
[38] Chen M, Zhou L, Wu Y, Zhao X and Zhang Y 2019 Rapid stress relaxation and moderate temperature of malleability enabled by the synergy of disulfide metathesis and carboxylate transesterification in epoxy vitrimers *ACS Macro Lett.* **8** 255–60
[39] Zhang Y H, Zhai M J, Shi L, Lei Q Y, Zhang S T, Zhang L, Lyu B, Zhao S H, Ma J Z and Thakur V K 2023 Sustainable castor oil-based vitrimers: towards new materials with reprocessability, self-healing, degradable and UV-blocking characteristics *Ind. Crops Prod.* **193** 116210
[40] ten Buren E B *et al* 2014 Toolkit for visualization of the cellular structure and organelles in *Aspergillus niger ACS Synth. Biol.* **3** 995–8
[41] Sánchez-Maldonado A F, Schieber A and Gänzle M G 2011 Structure–function relationships of the antibacterial activity of phenolic acids and their metabolism by lactic acid bacteria *J. Appl. Microbiol.* **111** 1176–84
[42] Shakhatreh M A K, Al-Smadi M L, Khabour O F, Shuaibu F A, Hussein E I and Alzoubi K H 2016 Study of the antibacterial and antifungal activities of synthetic benzyl bromides, ketones, and corresponding chalcone derivatives *Drug Des. Dev. Ther.* **10** 3653–60
[43] Olmos D and González-Benito J 2021 Polymeric materials with antibacterial activity: a review *Polymers* **13** 613
[44] Han J, Chen Q, Feng Y, Shen Y, Wu D, Zhong M, Zhang Q, Zhao Z, Zhai Y and Bockstaller M R 2023 Seawater-degradable and antibacterial epoxy thermosets employing betaine ester linkages *ACS Appl. Polym. Mater.* **5** 3298–305
[45] Wang Z, Zhang X, Yao W, Dong Y, Zhang B, Dong X, Fang H, Zhang G and Ding Y 2022 Dynamically cross-linked waterborne polyurethanes: transalkylation exchange of C–N bonds toward high performance and reprocessable thermosets *ACS Appl. Polym. Mater.* **4** 5920–6
[46] Yang Y, Xia Z, Huang L, Wu R, Niu Z, Fan W, Dai Q, He J and Bai C 2022 Renewable vanillin-based thermoplastic polybutadiene rubber: high strength, recyclability, self-welding, shape memory, and antibacterial properties *ACS Appl. Mater. Interfaces* **14** 47025–35
[47] Chen P, Liu Y, Li C, Hua S, Sun C and Huang L 2023 Antibacterial mechanism of vanillin against. Escherichia coli O157: H7 *Heliyon* **9** e19280
[48] Wang W, Chen Z Q, Lin B, Liu M C, Zhang Y, Liu S J, Li Y and Zhao Q 2024 Two-photon polymerization-based 3D micro-scaffolds toward biomedical devices *Chem. Eng. J.* **493** 152469
[49] Kumar A, Panda D and Gangawane K M 2024 *Microfabrication and Nanofabrication: Precision Manufacturing* (De Gruyter)